H_{inf} CONTROL APPLIED TO A ONE LINK FLEXIBLE MANIPULATOR

Celiane Costa Machado, dmtccm@furg.br
Sebastião Cícero Pinheiro Gomes, dmtscpg@furg.br
Fundação Universidade Federal do Rio Grande (FURG)
Núcleo de Matemática Aplicada e Controle
Av. Itália km 8, 96201-900, Rio Grande, RS

Álvaro Luiz de Bortoli, dbortoli@mat.ufrgs.br
Universidade Federal do Rio Grande do Sul (UFRGS)
Departamento de Matemática
Av. Bento Gonçalves, 9500, 91509-900, Porto Alegre, RS

Abstract. *This paper presents a control strategy based on the combination of the H_∞ synthesis with a bilinear transformation, whose purpose is to attenuate the structural vibrations in a flexible manipulator. The existence of actuator nonlinear friction, sometimes, annuls the torques produced by the control law due to torque dead zone, making the use of the control law non-viable. An important work of modeling based on experimental results was carried through in the present article. Open loop results showed simulations very closed to experimental results. H_∞ control was projected based on this model. Simulations results shows a good closed loop performance if the actuactor is considered as linear. However, when the actuctor dynamics is nonlinear (stick-slip and torque dead zone), the closed loop performance is significantly diminished.*

Keywords*: H_∞ control, flexible, manipulator, modeling, friction.*

1. INTRODUCTION

Friction is a phenomena present in almost all mechanical systems and constitutes one of the main causes of loss performance of the control law. Dynamic effects as torque dead zone and stick-slip behavior are very restrictives to the good performance of control laws. These problems are amplificated if the robot has flexible links, as wil be demonstrated in this paper.

Many papers have beem published on friction in robotics (Armonstrong-Helouvry, 1993), (Armonstrong-Helouvry et al., 1994), (Canudas et al., 1995), (Bensançom-Veda and Bensançon, 1999), (Ruy et al., 2001), (Huang et al., 2002) and (Gomes et al., 2003). The main approach is the proposal of friction models and compensation mechanisms. However, friction at low speeds (ocorrence of stick-slipe behavior) is very dificult to modeling, and, therefore, there are actuals works using artifitial neural network (NN) to friction modeling (Gomes, *et. al*., 2006). NN applications in science initiated approximately twenty five years ago, (Kaynak and Ertugru, 1997), (Jung and Hsia, 1998). However, friction modeling using NN are more recent (Dapper et al., 1999), (Selmic and Lewis, 2000). Mechanisms based on fuzzy and on neuro-fuzzy compensators are also used in friction compensation (Suraneni et al., 2005) and (Gomes *et al*., 2006).

In synthesis, to project control laws to flexible structures does not represent a challenge if the actuator has linear characteristics (direct drive, for example). However, the use of conventional actuators (harmonic-drive, for example) can completaly make impraticable the performance of the control laws. The main reason is that the torque calculated by the control law does not arrive until the structure due the friction torque dead zone. In the case of the flexible manipulator, the flexible beam reamains vibrating as it was fixed in one extremity and free in the other.

When control laws are projected to flexible manipulators, it is important to point out that, besides the inherent difficulty due friction phenomenon, it is importante to use robust control to deal with differences between nominal model and physical plant to project control laws with real condictions to experimental implementation. In this paper, a control law is presented: H_∞ with a bilinear transformation, that proved to be efficient in the structural vibration control of the flexible manipulator, if the actuator has linear behavior.

2. EXPERIMENTAL SETUP

It was constructed a flexible robot manipulator at the Applied Mathematics and Control Laboratory, located in the Federal University of Rio Grande, Brazil. In (Gomes *et al*., 2006) there are more general details about the robot design. A picture of this manipulator can be seen in Fig. 1. It is composed by a very flexible beam, made in aluminium, free at one extremity (end effector) and articulated at the other (motor with gear drive joint). Three strain gauges sensors were placed on the flexible beam and provided angular deformation measures at selected points, as will be explained in Section III. This number of strain gauges was used because the second flexible mode is well visible in the experiments and the interest is in the control of the two first flexible modes. There was also an encoder that provided the rotor

angular position. The physical parameters of the flexible manipulator are defined in the Table I (in this paper, all variables and parameters have physical units defined at the actuator load output axis side).

Table 1. Parameters of the flexible manipulator.

Parameter	Symbol	Valor
Elasticity	EI	$1.975 Nm^2$
Beam dimensions	l, h, e	$1.1m;\ 0.012m;\ 0.00305m$
Beam mass	m_b	$0.111178\ kg$

EI is the Young module multiplied by the straight section inertia, l, m_b , h and e are the length, mass, height and thickness of the flexible beam, respectively. In Fig. 2 there is a geometric representation of the flexible manipulator, indicating that the most important flexibility occurs on the horizontal plane (interest to the control). It was used a harmonic-drive actuator (Fig. 3). This type of actuator is very used in robotics because there is no considerable backlash. However, this actuator has an important torque dead zone due to the nonlinear friction. Table II shows the physical characteristics of the harmonic-drive used in this work. There is no difficulty to attenuate the structural vibrations using a direct drive, because this type of actuator has an insignificant torque dead zone. Nevertheless, there is no practical interest in using direct drive due to its little torque autonomy. The true challenge is to project control laws to attenuate the structural vibrations with actuators that use gearboxes. This is the reason to use a harmonic-drive in the present research.

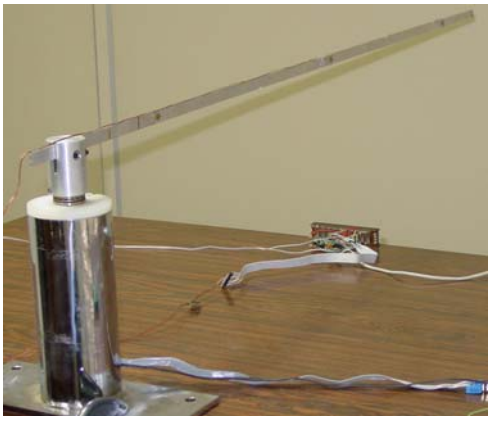

Fig. 1 Photography of the flexible manipulator.

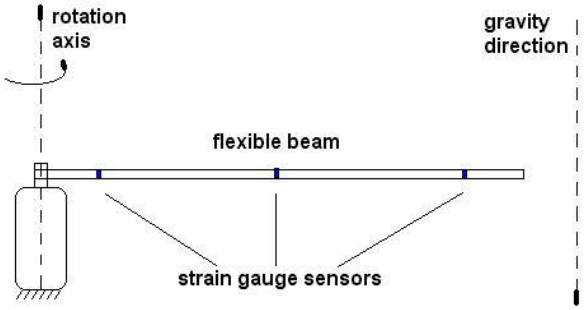

Figure 2. Geometric representation of the flexible manipulator.

Figure 3. A photograph of the actuator.

Table 2. Physical parameters of the actuator.

Parameter	Symbol	Valor
Rotor inertia	I_r	$0.01334 kgm^2$
Gear ratio	η	100
Torque/current constant	*Tcc*	$1.74 Nm/A$
Encoder resolution	*Res*	$500 PPR$

A dedicated hardware was built using the harmonic-drive based actuator, a personal computer and an interface module, in order to obtain the experimental results (Fig 4).

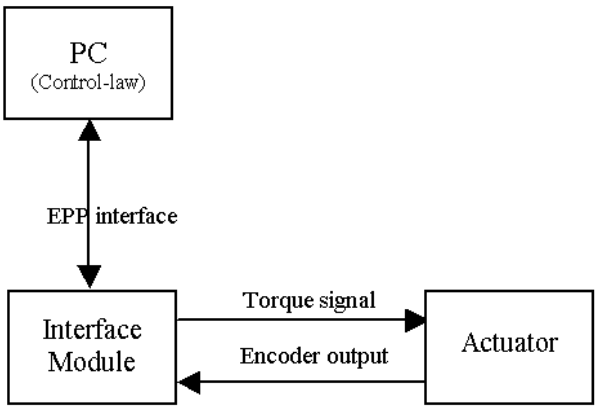

Fig 4. Top-level diagram of the control system.

As one can see in Fig 4, the PC is connected to a dedicated interface module using PC's parallel port (printer port) in EPP mode, which is bi-directional. The Interface Module is composed by a FPGA (Field Programmable Gate Array) and a driver interface. The FPGA condenses all the logic necessary to implement an EPP interface, an incremental encoder interface and a PWM (Pulse Width Modulation) generator. The driver interface then converts the PWM signal coming from the FPGA in a current signal to drive the DC motor of the actuator, producing a torque proportional to the applied current. A software driver written in C language for DOS makes available the position (rad) and velocity (rad/s) to the control-law and sends the torque calculated by the control-law to the actuator.

3. DYNAMIC MODEL

The dynamic model of the manipulator is constituted by the models of the actuator and the flexible structure. The actuator model considered in this study was proposed by Gomes and Rosa, 2003 and the structural model was proposed by Machado et al., 2002. The main elements considered in each model are described below.

3.1 Actuator model

The considered robotic actuator adds a vibration mode due to internal elasticity, whose frequency is higher than the third structure vibration mode, allowing that a rigid aproximation to the actuator in this case. The equation that represents the actuator dynamics is:

$$I_t \ddot{\theta}_r + f_v^* \dot{\theta}_r = T_m - T_l \tag{1}$$

where I_t is the total inertia (rotor plus the base connected to the gear output), f_v^* is the variable viscous friction coefficient (Gomes and Rosa, 2003), θ_r is the rotor angular position, T_m is the motor torque and T_l is the set of possible external torques applied to the load coupled to the gear output axis. To consider non linearity related to the physical phenomenon, such as stick-slip modes and Stribeck effect (Gomes et al., 2006), the coefficient f_v^* is function both of the state vector and the motor torque. When the objective is to work with linear dynamics for the friction, it is enough to adopt a constant value for f_v^*, equal to the coefficient of the average viscous friction.

3.2 Structural model

The structural model was originally considered in Machado et al., 2002; it approaches continuous flexibility in a discrete way by introducing fictitious joints of elastic constants $\alpha_i k$, located according to the rule presented in Fig. 5. The use of n fictitious joints means the consideration of n flexible modes in the structural model. Constant $k = \frac{nEI}{l}$ is adopted, where l is the beam length. The constants $\alpha_i\,(i = 1,...,n)$ are determined by forcing the model frequencies to coincide with the frequencies analytically predicted (Pereira, 1999) or with the experimentally identified ones.

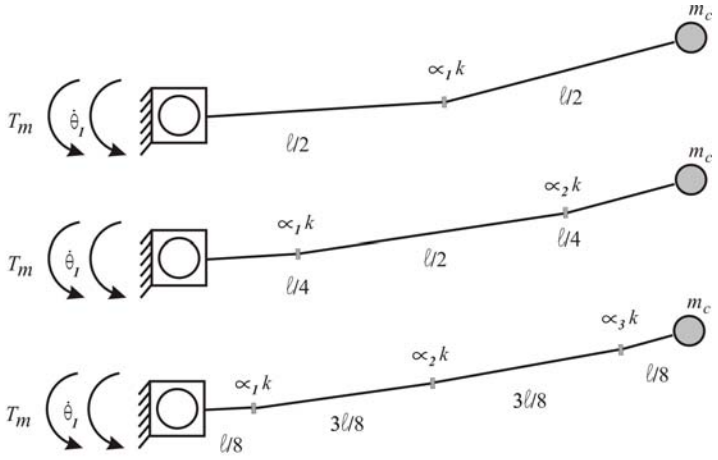

Fig. 5 Discrete approach for continuous flexibility.

After locating the fictitious joints, supposing that *l* is the structure length, knowing the masses of every rigid element (concentrated in respective mass centers), the mass of the terminal load and the elastic constants of every fictitious joint, and considering θ_i the angle between direction *x* and the respective rigid element of number *i*, the kinetic and potential energies and, consequently, the Lagrangian system are obtained. By means of the Euler-Lagrangian equations and also, considering small angular deformations in the fictitious joints, the dynamic model can be written as:

$$[I_{in}]\ddot{\vec{\theta}} + [C_{at}]\dot{\vec{\theta}} + [K_{el}]\vec{\theta} = B' T_m \tag{2}$$

where *n* is the number of fictitious joints, $[I_{in}]_{n+1xn+1}$ is the inertia matrix, $[K_{el}]_{n+1xn+1}$ is the elastic constant matrix, $[C_{at}]_{n+1xn+1}$ is the friction matrix and $B' = [1 \;\; 0 \;\; \cdots \;\; 0]^T$. In Machado *et al.* (2002), a methodology for direct obtention of the matrices I_{in} , C_{at} and K_{el} is presented. The global dynamic model of the manipulator, including the actuator and the flexible structure dynamics, can be written in the state space form $\dot{\vec{X}} = A\vec{X} + BT_m$, considering actuator linear friction approximation and in the form $\dot{\vec{X}} = A(\vec{X}, T_m)\vec{X} + BT_m$, when the non linear friction in the actuator is considered. It is important to point out that the used modeling process considers the state variables related to the inertial frame. As the strain-gauges sensors supply the angular deformation measures at the fictitious joints positions, the state variables may be extracted from these observations, as following:

$$\theta_r \Rightarrow \textbf{encoder signal;} \qquad \theta_1 = \theta_r + e_1;\; \theta_2 = \theta_1 + e_2;\; \theta_3 = \theta_2 + e_3;$$

where e_1, e_2 and e_3 are obtained from the strain-gauges measures 1, 2 and 3, respectively. The angular velocities were obtained by online time derivative of the angular positions.

4. EXPERIMENTAL OPEN LOOP RESULTS

The static friction torque was identified as being equivalent to 10.8% of the maximum actuator motor torque and this limit defines the torque dead zone. It means that any torque below 10.8% of the maximum motor torque will not generate motion of the actuator load output axis. Fig. 6 shows an experimental result to illustrate this fact. A motor torque equal to 50% of the maximum motor torque was applied during 0.05*s*. After this time the same step in torque was applied in the negative sense during 0.05*s*. After 0.1*s*, the motor torque was annulled. Fig. 6 shows, at its upper

part, the structural reaction torque (load torque T_l, estimated with the first strain-gauge signal) applied at the actuator load output axis and also the positive and negative static friction levels, pointing out the torque dead zone. It is evident that, in most part of the time, the structural reaction torque is into the torque dead zone. As the control torque needed to attenuate the structural vibration has amplitude level equivalent to the structural reaction torque amplitude, this means that while the torque dead zone problem exists, it is not possible to attenuate the structural vibrations with active control.

Fig. 7 shows a confrontation between simulation and experiment in open loop. It was applied a step motor torque equal to 50% of the maximum torque at the first 0.05*s*, -50% at the following 0.05*s* and a null torque up to 0.1*s*. The simulation and the equivalent experimental results are plotted in Fig. 7, showing the tip angular position (θ_3). In this figure is also shown a zoom related to the first three seconds and the difference between experimental and simulation results (error). The simulation was performed using the f_v^* in $[C_{at}]$ matrix. It can be seen that the dynamic model (structure and actuator) well reproduce the experimental result, in which it is quit visible the two first structural flexible modes. These modes have the cantilevers frequencies, equivalent to the zeros frequencies of the collocated open loop transfer function (Pereira, 1999). When the actuator is in stick mode, the rotor is locked (the rotor velocity is zero) and this means that the dynamic system vibrates with the cantilevers modes. The open loop poles and zeros are showed in Table III. The lowest observed frequency in the experimental result in Fig. 7 corresponds to 12.1 *rd/s*.

Table 3. Open loop poles and zeros

zeros	-0.0057±12.1*i*; -0.658±76.19*i*; -4.169±247.89*i*
poles	0; -1.78; -2.55±23.6*i*; -0.87±78.72*i*; -4.35±249.99*i*

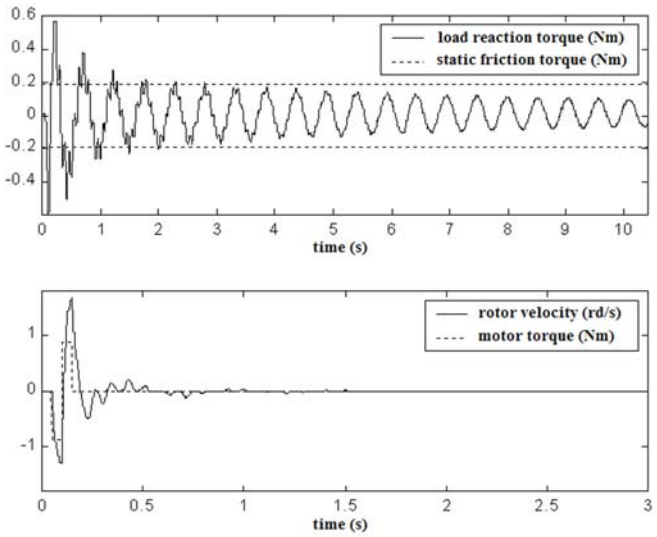

Fig. 6. Experimental results with open loop flexible modes activation.

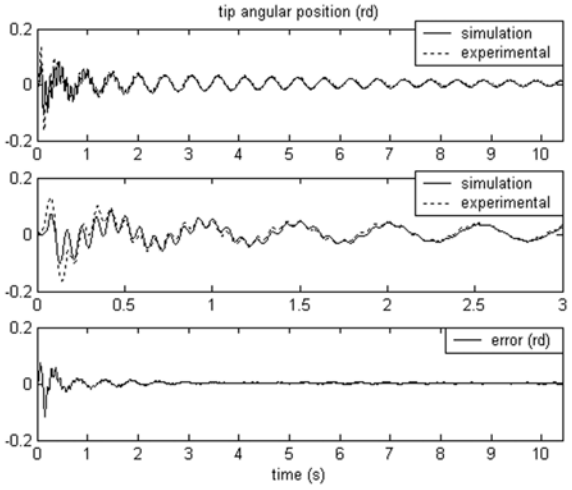

Fig. 7 Oppen loop comparisons between experimental and simulation results.

5. CONTROL LAW

The control law consists of a combination of the H_∞ synthesis and a bilinear transformation (Chiang and Safanov, 1992). A linear approach for the actuator was considered, with $f_v^* = c_r = 0.278 Nms/rd$ (average viscous friction coefficient in the actuator). The state vector has the following form

$$\vec{x} = \begin{bmatrix} \theta_r & \theta_1 & \theta_2 & \theta_3 & \dot{\theta}_r & \dot{\theta}_r & \dot{\theta}_2 & \dot{\theta}_3 \end{bmatrix}^T$$

where θ_r, θ_1, θ_2, θ_3 are the angular positions of the rotor and the fictitious joints 1, 2 and 3, respectively.

The control law was mainly projected to attenuate the first vibration mode, i.e., a high performance level was not required to guarantee stability. The control law project consists of a combination of a bilinear transformation and the synthesis H_∞ (Chiang and Safanov, 1992), where the bilinear transformation aims at removing the bad conditioning in the augmented plant.

5.1 H_∞ synthesis

The system described by the block diagram (Fig. 8) is considered, where $P(s)$ (transfer function of the augmented plant) and $K(s)$ (transfer function of the compensator) are proper and rational functions.

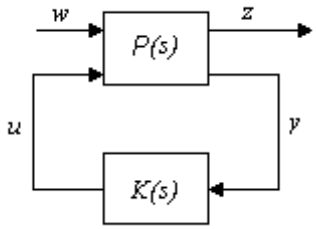

Figure 8. Standard block diagram.

Vector *w* represents an input signal; u is the vector of the controller $K(s)$; z is the output vector of the augmented plant and y is the vector of the sensor mesures.

The control problem consists of determining a stabilizing law

$$u(s) = K(s)y(s) \tag{3}$$

so that the H_∞ norm of the transfer matrix from *w* to z is minimized.

The augmented plant $P(s)$ can be written in the following form:

$$P(s) = \begin{bmatrix} P_{11} & P_{12} \\ P_{21} & P_{22} \end{bmatrix} = \begin{bmatrix} [A] & \begin{bmatrix} B_1 & B_2 \end{bmatrix} \\ \begin{bmatrix} C_1 \\ C_2 \end{bmatrix} & \begin{bmatrix} D_{11} & D_{12} \\ D_{21} & D_{22} \end{bmatrix} \end{bmatrix}$$

or

$$\begin{aligned} \dot{x} &= Ax + B_1 w + B_2 u \\ z &= C_1 x + D_{11} w + D_{12} u \\ y &= C_2 x + D_{21} w + D_{22} u \end{aligned} \quad , \tag{4}$$

where $z(t) \in R^{p_1}$, $y(t) \in R^{p_2}$, $w(t) \in R^{m_1}$, $u(t) \in R^{m_2}$ and $x(t) \in R^n$.

It can be written

$$P_{ij} = C_i (sI - A)^{-1} B_j + D_{ij} ,$$

$$\begin{bmatrix} z \\ y \end{bmatrix} = \begin{bmatrix} P_{11} & P_{12} \\ P_{21} & P_{22} \end{bmatrix} \begin{bmatrix} w \\ u \end{bmatrix} ,$$

where $s = j\omega$ and ω represents the frequency.

Considering equations (3) and (4), the transfer function from w to z, T_{zw}, can be obtained. It is also called lower linear fractional transformation (LFT) and has the form:

$$T_{zw} = F_l(P,K) = P_{11} + P_{12}K(I - P_{22}K)^{-1}P_{21}.$$

Therefore, the H_∞ optimal control problem consists of the minimization of $\|F_l(P,K)\|_\infty$ in the space of all controllers $K(s)$ which stabilize the system. In case $\|F_l(P,K)\|_\infty < \gamma$, for $\gamma > 0$, it is said that the controller $K(s)$ is suboptimal.

Assuming that the following conditions are valid:
(a1) (A,B_2) is stabilizable and (C_2,A) is detectable;

(a2) $D_{12} = \begin{bmatrix} 0 \\ I \end{bmatrix}$ and $D_{21} = \begin{bmatrix} 0 & I \end{bmatrix}$;

(a3) $\begin{bmatrix} A - j\omega I & B_2 \\ C_1 & D_{12} \end{bmatrix}$ has full column rank $\forall\,\omega$;

(a4) $\begin{bmatrix} A - j\omega I & B_1 \\ C_2 & D_{21} \end{bmatrix}$ has full row rank $\forall\,\omega$.

The solution to this control problem involves the resolution of two algebraic Riccati equations, (Doyle et al., 1989) and (Zhou and Doyle, 1996); each one of same order of the augmented plant P. The "*hinf.m*" function of the MATLAB implements a solution to this problem.

5.2 Augmented plant

The augmented plant was obtained considering the formulation presented in Fig. 9, taking in to account the existence of three fictitious joints, whereas the controller transfer function was obtained with the function "*hinf.m*" of the MATLAB (Chiang and Safanov, 1992).

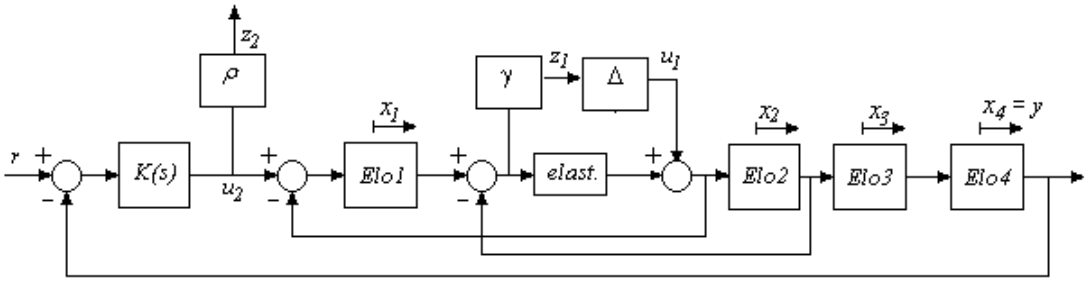

Fig. 9 Block diagram of the augmented plant.

The augmented plant is written in the form:

$$\dot{x} = Ax + B_1u_1 + B_2u_2$$
$$z = C_1x + D_{11}u_1 + D_{12}u_2$$
$$y = C_2x + D_{21}u_1 + D_{22}u_2$$

whre x is the system state vector (positions and velocities),

$$A = \begin{bmatrix} 0_{4\times4} & I_{4\times4} \\ -I_{in}^{-1}K_{el} & -I_{in}^{-1}C_{at} \end{bmatrix}, \quad B_1 = \begin{bmatrix} 0_{4\times1} \\ I_{in}^{-1}\begin{bmatrix} -1 & 1 & 0 & 0 \end{bmatrix}^T \end{bmatrix}, \quad B_2 = \begin{bmatrix} 0_{4\times1} \\ I_{in}^{-1}\begin{bmatrix} 1 & 0 & 0 & 0 \end{bmatrix}^T \end{bmatrix}$$

$$z = \begin{bmatrix} z_1 & z_2 \end{bmatrix}^T$$

$$C_1 = \gamma \begin{bmatrix} 1 & -1 & 0 & 0 & 0 & 0 & 0 & 0 \\ 0 & 0 & 0 & 0 & 0 & 0 & 0 & 0 \end{bmatrix}, \quad D_{11} = \begin{bmatrix} 0 \\ 0 \end{bmatrix}, \quad D_{12} = \begin{bmatrix} 0 \\ \rho \end{bmatrix}$$

$$C_2 = \begin{bmatrix} 1 & 0 & 0 & 0 & 0 & 0 & 0 & 0 \end{bmatrix}, \quad D_{21} = 0 \text{ e } D_{22} = 0.$$

ρ represents a weigh on the signal control, γ a weigh on the structural elasticity and Δ is the uncertainty level ($\|\Delta\|_\infty \leq 1$).

The objective of the project is to find a control law that:

i. stabilizes the system, exactly admitting a variation on the elasticity in the first joint;
ii. attenuates the vibrations in a specified maximum time;
iii. keeps the control torque between daily established limits.

Thus, the control problem needs to satisfy the condition:

$$\left\| \begin{matrix} \gamma T_{z_1 u_1} \\ \rho T_{z_2 u_2} \end{matrix} \right\|_\infty < 1$$

6. SIMULATION RESULTS

Simulation results regarding the control law that combines the synthesis H_∞ and a bilinear transformation (Chiang and Safanov, 1992) applied to the flexible manipulator are shown below, where the resulting control law consists of a suboptimal solution to the control problem H_∞.

The bilinear transformation maps plan s on plan $\tilde{s}$, such that:

$$s = \frac{\tilde{s} + p_1}{\frac{\tilde{s}}{p_2} + 1}, \tag{5}$$

points p_1 and p_2 are the extremities of the diameter of a circle in the left semi-plan of s - plan.

The project procedure is summarized below:

i. The uncertainty block for the formulation of H_∞ robust control problem is stipulated (parameters ρ and γ);
ii. The plant of the s-plan is mapped on the $\tilde{s}$-plan by bilinear transformation (Eq. (5), parameters p_1 and p_2);
iii. The H_∞ controller for the transformed plant is calculated;
iv. The $\tilde{K}(s)$ controller is mapped back to the s-plan by inverse bilinear transformation of Eq. (5);
v. Step 2 is repeated and parameters p_1 and p_2 are adjusted until the desired result is obtained.

The results consider two situations: linear and nonlinear friction for the actuator dynamics. In the linear case, only a constant viscous friction coefficient is considered, whereas, and in the nonlinear case the friction model explained in section 3 is used. In both cases it was applied 100% of the maximum motor torque during 0.05*s*, -100% of this maximum torque in the following 0.05*s* and a null motor torque after 0.1*s*, in the case of open loop response. To closed loop response, the control is activated from 0.2s.

Fig. 10 shows open and closed loop results to the case of linear friction. The vibrations are attenuated 0.5*s* after the time of the beginning of the closed loop, as it can be visualized in the load angular position and velocity.

Fig. 11 shows open and closed loop results to the case of nonlinear friction. In this situation, the control law does not attenuate the vibrations and the performance is unacceptable. It is important to observe that the torque calculated by the control law remains inside of the torque dead zone, delimited by the horizontal hatched lines (in red in the graph of the motor torque). This means that the control torque does not reach the flexible structure, which remains vibrating, as a beam, fixed at one extremity and free at the other.

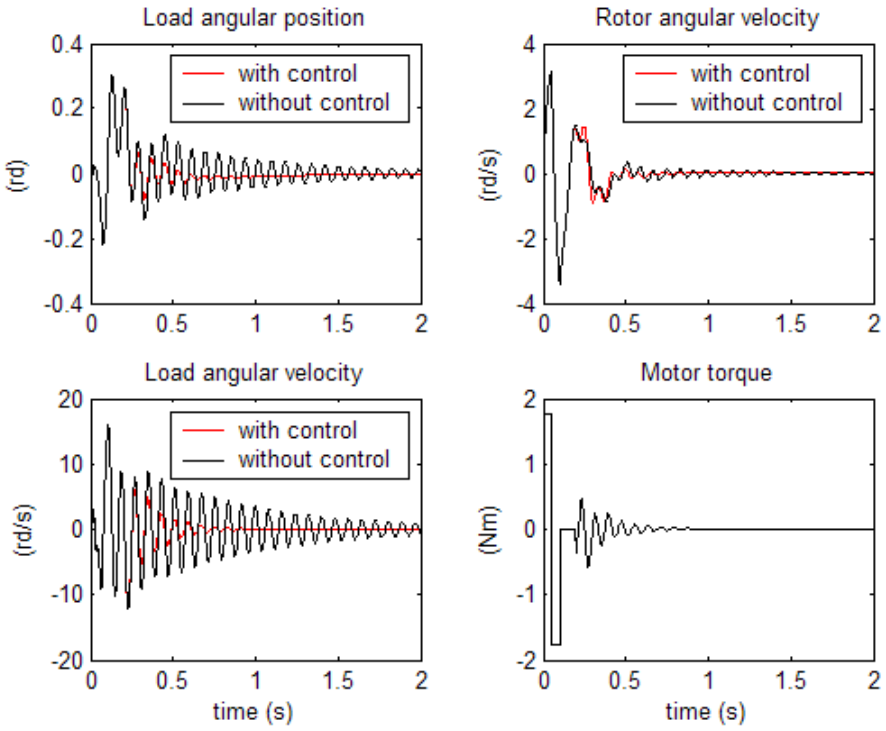

Fig. 10 Open and closed loop responses considering linear actuator dynamics.

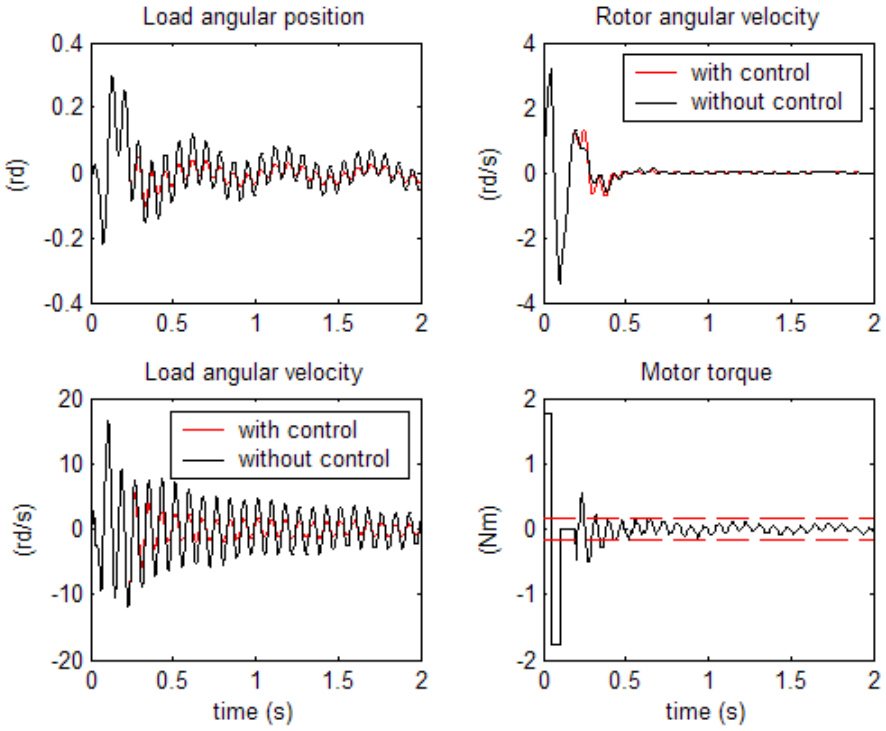

Fig. 11 Open and closed loop responses considering nonlinear actuator dynamics.

7. CONCLUSIONS

In the present article the possibility of control of a manipulator with an only flexible link was evaluated, using a synthesis of H_∞ control. Simulations had shown that, when the dynamics of the actuator is linear, it really does not have a problem, still when consider parametric variations in the structural elasticity. The project of control with robustness characteristics allows good results in the attenuation of the vibrations. However, when the nonlinear dynamics of the actuator is considered, the control law does not attenuate the vibrations. It is evident that, in most part of the time, the control law torque is into the torque dead zone and this means that while the torque dead zone problem exists, it is not possible to attenuate the structural vibrations with active control. To get this conclusion the knowledge of a realistic and preditivo dynamic model was imposing. Therefore, an important work of modeling based on experimental results was carried through in the present article. Future works will involve friction compensation mechanisms based on artificial neural networks and fuzzy systems, which will be used in parallel with robust control.

8. REFERENCES

Armstrong-Helouvry, B., (1993). Stick slip and control in low-speed motion. IEEE Transaction on Automatic Control, 38 (10), 1483-1496.

Armstrong-Helouvry, B., Dupont, P. E. and Canudas de Wit, C. (1994). A survey of analysis tools and compensation methods for control of machines with friction. Automatica, 30 (7), 1083-1138.

Beale, R. and Jackson, T. (1991). Neural computing: an introduction. Adam Higler Bristol.

Besançon-Veda, A. and Besançon, G. (1999). Analysis of a two-relay system configuration with application to Coulomb friction identification. Automática, 35 (8), 1391-1399.

Canudas de Wit, C., Astrom, K. J. and Lischinsky, P. (1995). A new model for control of systems with friction. IEEE Transaction on Automatic Control, 40 (3), 419-425.

Chiang, R. Y., Safonov, M. G. (1992). Robust Control Toolbox User's Guide. Math Words, South Natick.

Dapper, M., Zanh, V., Maass, R. and Ekmiller, R. (1999). How to compensate stick-slip friction in neural velocity force control (NVFC) for industrial manipulators. In IEEE Robotic and Automation Conference, Detroit, USA.

Doyle, J. C., Glover, K., Khargonekar, P. P. and Francis, B. A. (1989). State-space solutions to standard H_2 and H_{inf} control problems. IEEE Transaction on Automatic Control, 34, 831-847.

Fausett, L. (1994). Fundamentals of neural networks. Prentice Hall, New Jersey.

Gervini, V. I., Gomes S. C. P. and Rosa, V. S. (2003). A new robotic drive joint friction compensation mechanism using neural networks. Jornal of the Brazilian Society of Mechanical Science & Engineering, ABCM, April-June, XXV (2).

Gomes, S. C. P. and Rosa, V. S. (2003). A new approach to compensate friction in robotic actuators. In Proceedings of IEEE International Conference on Robotics and Automation (ICRA2003), Taipei, Taiwan.

Gomes, S. C. P., Rosa, V. S. and Albertini, B. C. (2006). Active control to flexible manipulators. IEEE/ASME, Transactions on Mechatronics, 11 (1), 75-83, USA.

Huang, S. N., Tan, K. K. and Lee, T. H. (2002). Adaptive motion control using neural network approximations. Automatica, 38, 227-233.

Jung, S. and Hsia, T. C. (1998). Analysis of nonlinear neural network impedance force control for robot manipulator. In IEEE Robotic and Automation Conference, Leuven, Belgium.

Kaynak, O. and Ertugru, M. (1997). Neural network adaptive sliding mode control and its application to SCARA type robot manipulator. In IEEE Robotic and Automation Conference, Albuquerque, New Mexico, USA.

Machado, C. C., Gomes, S. C. P., Pereira, A. E. L., Bortoli, A. L. (2002),Um novo algoritmo para a modelagem dinâmica de manipuladores flexíveis. Revista Controle e Automação, Vol 13, 134-140.

Pereira, A. E. L., (1999). Um Estudo Sobre Modelagem Matemática de Estruturas Flexíveis, Dissertação de Mestrado, UFRGS, Porto Alegre, Brasil.

Ryu, J., Song, J. and Kwon, D., (2001). A nonlinear friction compensation method using adaptive control and its practical application to an in-parallel actuated 6-DOF manipulator. Control Engineering Practice, 9, 159-167.

Selmic, R. R. and Lewis, F. L. (2000). Dead zone compensation in motion control systems using Neural Networks. IEEE Transactions on Automatic Control, 45.

Suraneni, S., Kar, I. N., Ramana Murthy, O. V. and Bhatt, R. K. P. (2005). Adaptive stick-slip and backlash compensation using dynamic fuzzy logic system. Applied Soft Computing, 6, 26-37.

Zhou, K., Doyle, J. C. and Glover, K. (1996). Robust and optimal control. Prentice Hall, New Jersey.